

Strong gravitational lensing constraints on holographic dark energy

Jing-Lei Cui,¹ Yue-Yao Xu,¹ Jing-Fei Zhang,¹ and Xin Zhang^{*1,2, †}

¹*Department of Physics, College of Sciences, Northeastern University, Shenyang 110819, China*

²*Center for High Energy Physics, Peking University, Beijing 100080, China*

Strong gravitational lensing (SGL) has provided an important tool for probing galaxies and cosmology. In this paper, we use the SGL data to constrain the holographic dark energy model, as well as models that have the same parameter number, such as the w CDM and Ricci dark energy models. We find that only using SGL is difficult to effectively constrain the model parameters. However, when the SGL data are combined with CBS (CMB+BAO+SN) data, the reasonable estimations can be given and the constraint precision is improved to a certain extent, relative to the case of CBS only. Therefore, SGL is an useful way to tighten constraints on model parameters.

PACS numbers: 95.36.+x, 98.80.Es, 98.80.-k

Keywords: cosmological constraints, strong gravitational lensing, holographic dark energy

1. Introduction

Dark energy (DE) has been proposed to explain the accelerating expansion of the universe found by various observations [1–5]. We actually know little about its nature other than the fact that it is gravitationally repulsive and contributes about 70% of the cosmic energy density. Many cosmologists suspect that the identity of DE is the cosmological constant, and the corresponding DE model is dubbed as Λ CDM, which fits the observational data quite well. However, the Λ CDM model confronts with the severe theoretical problems, i.e., “fine-tuning” and “cosmic coincidence” puzzles [6–11]. Hence, cosmologists constructed a host of theoretical/phenomenological DE models [12–28] in terms of the physics different from Λ CDM. For the recent progress in DE field, see, e.g., [29–39].

The holographic dark energy (HDE) model [40] is a dynamical DE model based on the holographic principle. Cohen et al. [41] pointed out that the total energy of a system with size L should not exceed the mass of a black hole with the same size, i.e., $L^3\rho_{\text{de}} \lesssim LM_{\text{P}}^2$. This energy bound leads to the density of holographic dark energy,

$$\rho_{\text{de}} = 3c^2 M_{\text{P}}^2 L^{-2}, \quad (1)$$

where c is a dimensionless parameter characterizing some uncertainties in the effective quantum field theory, M_{P} is the reduced Planck mass defined by $M_{\text{P}}^2 = (8\pi G)^{-1}$, and L is the infrared (IR) cutoff in the theory. Li [40] suggested that the IR cutoff L should be given by the event horizon of the universe, defined as

$$L = a(t) \int_t^{\infty} \frac{dt'}{a(t')} = a \int_a^{\infty} \frac{da'}{Ha'^2}, \quad (2)$$

where a is the scale factor of our universe, the Hubble parameter $H = \dot{a}/a$, and the dot denotes the derivative with respect to time t . This yields the HDE model studied in this paper,

which is a very competitive candidate for DE, attracting lots of studies [42–52].

To constrain the parameter space of various DE models, the observational data including cosmic microwave background (CMB), baryon acoustic oscillations (BAO), type Ia supernova (SN) and so on, have been used [53–64]. However, to obtain tighter constraints on parameters, we need more cosmological probes, for example, the strong gravitational lensing (SGL). SGL can provide the information about the proper angular diameter distances between lens and source and between observer and source. Since these distances depend on cosmological geometry, we can use their ratio to constrain the parameters in cosmological model. Furthermore, the strong lens systems produced by massive galaxies are fairly useful to constrain the statistical properties of galaxies. After the pioneer SGL in Q0957+561 [65] was discovered, SGL has increased to enough number and developed into an important astrophysical tool for probing both galaxies (their structure, formation and evolution) [66–72] and cosmology [73–80].

In this paper, we constrain the HDE model with 73 gravitational lens data points from Sloan Lens ACS (SLACS) and Lens Structure and Dynamics (LSD) survey released in Ref. [81], which were also used in the constraints on the $f(R)$ [82], $f(T)$ [83] and ϕ CDM [84] models. Besides, the combination of SGL with other geometrical measurements including CMB, BAO and SN (together as “CBS”) is also considered. Furthermore, for comparison, we also constrain other DE models with the same parameter number, such as w CDM (with the constant equation of state w) and Ricci dark energy (RDE) [85] models, by using the same data.

We arrange the paper as follows. In Sec. 2, we briefly introduce the data and analysis methods. We present the constraint results of the HDE model in Secs. 3. The constraint results of the other two models are presented in Sec. 4. The conclusion is shown in Sec. 5.

2. Data and analysis methods

In this section, we describe the observational data used in this paper, including SGL, CMB, BAO and SN. We first give

*Corresponding author

†Electronic address: zhangxin@mail.neu.edu.cn

the definitions of the proper angular diameter distance $D_A(z)$ and luminosity distance $D_L(z)$, due to their significance in the geometrical probes. In a spatially flat Friedmann-Robertson-Walker (FRW) universe, we have

$$D_A(z) = \frac{1}{H_0(1+z)} \int_0^z \frac{dz'}{E(z')}, \quad (3)$$

$$D_L(z) = \frac{(1+z)}{H_0} \int_0^z \frac{dz'}{E(z')}, \quad (4)$$

where $E(z) \equiv H/H_0$ is the dimensionless Hubble expansion rate.

2.1 Strong gravitational lensing

Gravitational lensing effect refers to that light rays from a distant quasar or galaxy to us will be bent when they travel through gravitational field given by galaxy or galaxy cluster acting as lens. Strong lensing is to produce multiple images of the source, arcs or even Einstein rings. In the lensing analyses, the Einstein radius (θ_E) is a basic quantity. The formula of θ_E in a lensing system modeled by the singular isothermal sphere (SIS) assumption can be expressed as

$$\theta_E = 4\pi\sigma_{\text{SIS}}^2 \frac{D_A(z_l, z_s)}{D_A(0, z_s)}, \quad (5)$$

where $D_A(z_l, z_s)$ and $D_A(0, z_s)$ are the proper angular diameter distances between lens and source and between observer and source respectively, which can be calculated according to Eq. (3), and σ_{SIS} is the velocity dispersion of the SIS model. Obviously, according to the distance ratio $D_A(z_l, z_s)/D_A(0, z_s)$, the Einstein radius is dependent on the cosmological model and independent on the Hubble constant value. Thus, we can estimate the parameters of the cosmological model through the distance ratio

$$\mathcal{D}(z_l, z_s) = \frac{D_A(z_l, z_s)}{D_A(0, z_s)} = \frac{\int_{z_l}^{z_s} dz'/E(z')}{\int_0^{z_s} dz'/E(z')}. \quad (6)$$

In Table 1 of Ref. [81], 80 data points are listed, including the redshifts of lens and source, z_l and z_s , as well as the observational \mathcal{D}^{obs} and its corresponding uncertainty $\sigma_{\mathcal{D}}$. In these data, 70 strong lensing systems come from SLACS and LSD survey, and 10 giant arcs samples come from galaxy clusters in the redshift region from 0.1 to 0.6. We select 73 observational data with the selection criterion $\mathcal{D}^{\text{obs}} < 1$ from Table 1 of Ref. [81], which means that the distance between the lens and source should be always smaller than that between the source and observer. Then we use these data to constrain the parameters of DE models by minimizing the following χ^2 function,

$$\chi_{\text{SGL}}^2 = \sum_i \frac{(\mathcal{D}_i^{\text{th}} - \mathcal{D}_i^{\text{obs}})^2}{\sigma_{\mathcal{D},i}^2}. \quad (7)$$

2.2 Cosmic microwave background

For CMB data, we use the distance prior data extracted from Planck first data release [86]. The distance priors include the shift parameter R , the acoustic scale ℓ_A and $\omega_b \equiv \Omega_{\text{b}0}h^2$. R and ℓ_A are, respectively, defined as

$$R \equiv \sqrt{\Omega_{\text{m}0}H_0^2(1+z_*)}D_A(z_*) \quad (8)$$

and

$$\ell_A \equiv (1+z_*) \frac{\pi D_A(z_*)}{r_s(z_*)}, \quad (9)$$

where $\Omega_{\text{m}0}$ is the present-day fractional energy density of matter, $D_A(z_*)$ is the proper angular diameter distance at the redshift of the decoupling epoch of photon z_* , and $r_s(z_*)$ is the comoving sound horizon at z_* . Here, $r_s(z)$ is given by

$$r_s(z) = H_0^{-1} \int_0^a \frac{da'}{a'^2 E(a') \sqrt{3(1+\bar{R}_b a')}}}, \quad (10)$$

where $\bar{R}_b a = 3\rho_b/(4\rho_\gamma)$ with ρ_b and ρ_γ being the baryon and photon energy densities, respectively. Thus we have $\bar{R}_b = 31500\Omega_{\text{b}0}h^2(T_{\text{cmb}}/2.7\text{K})^{-4}$, where $\Omega_{\text{b}0}$ is the present-day fractional energy density of baryon, h is the reduced Hubble constant defined by $H = 100h$ km/s/Mpc, and $T_{\text{cmb}} = 2.7255\text{K}$. z_* is given by the fitting formula [87],

$$z_* = 1048[1 + 0.00124(\Omega_{\text{b}0}h^2)^{-0.738}][1 + g_1(\Omega_{\text{m}0}h^2)^{g_2}], \quad (11)$$

where

$$g_1 = \frac{0.0783(\Omega_{\text{b}0}h^2)^{-0.238}}{1 + 39.5(\Omega_{\text{b}0}h^2)^{-0.763}}, \quad g_2 = \frac{0.560}{1 + 21.1(\Omega_{\text{b}0}h^2)^{1.81}}. \quad (12)$$

We use the mean values and covariance matrix of $\{\ell_A, R, \omega_b\}$ in [86] obtained from the Planck+lensing+WP data. The χ^2 function for CMB is

$$\chi_{\text{CMB}}^2 = \Delta p_i [\text{Cov}_{\text{CMB}}^{-1}(p_i, p_j)] \Delta p_j, \quad \Delta p_i = p_i^{\text{th}} - p_i^{\text{obs}}, \quad (13)$$

where $p_1 = \ell_A$, $p_2 = R$ and $p_3 = \omega_b$.

2.3 Baryon acoustic oscillations

In BAO measurements, the ratio of the effective distance measures $D_V(z)$ and $r_s(z_d)$ can be provided. The spherical average gives us the expression of $D_V(z)$,

$$D_V(z) \equiv \left[(1+z)^2 D_A^2(z) \frac{z}{H(z)} \right]^{1/3}. \quad (14)$$

$r_s(z_d)$ can be calculated by using Eq. (10), and z_d denotes the redshift of the drag epoch, whose fitting formula is given by [88],

$$z_d = \frac{1291(\Omega_{\text{m}0}h^2)^{0.251}}{1 + 0.659(\Omega_{\text{m}0}h^2)^{0.828}} [1 + b_1(\Omega_{\text{b}0}h^2)^{b_2}], \quad (15)$$

TABLE I: Constraint results and corresponding χ^2_{\min} for the HDE model by using the SGL and CBS (CMB+BAO+SN) data, as well as the combination of them. In the case of fixed Ω_{m0} , we choose $\Omega_{m0} = 0.27$.

Parameter	Ω_{m0}	c	χ^2_{\min}
SGL (Ω_{m0} free)	$0.0244^{+0.1123}_{-0.0136}$	$1.9730^{+0.0270}_{-0.8993}$	84.1185
SGL (Ω_{m0} fixed)	0.27	$0.8335^{+0.8031}_{-0.3495}$	87.2689
CBS	$0.2798^{+0.0083}_{-0.0114}$	$0.6458^{+0.0472}_{-0.0483}$	430.0321
SGL+CBS	$0.2783^{+0.0092}_{-0.0100}$	$0.6429^{+0.0515}_{-0.0436}$	517.6995

where

$$b_1 = 0.313(\Omega_{m0}h^2)^{-0.419}[1 + 0.607(\Omega_{m0}h^2)^{0.674}], \quad (16)$$

$$b_2 = 0.238(\Omega_{m0}h^2)^{0.223}.$$

We use 7 BAO data points from the 6dF Galaxy Survey [89], the SDSS-DR7 [89], the BOSS-DR11 [90] and the ‘‘improved’’ WiggleZ Dark Energy Survey [91]. The χ^2 function for BAO is

$$\chi^2_{\text{BAO}} = \Delta p_i [\text{Cov}_{\text{BAO}}^{-1}(p_i, p_j)] \Delta p_j, \quad \Delta p_i = p_i^{\text{th}} - p_i^{\text{obs}}. \quad (17)$$

Note that three WiggleZ data are correlated with each other, and the inverse covariance matrix for them is given in [91].

2.4 Type Ia supernova

We choose to use the first three-year dataset of the Supernova Legacy Survey (SNLS3) consisting of 472 SN [92]. SN Ia data give measurements of the luminosity distance $D_L(z)$ through that of the distance modulus of each SN. The predicted magnitude of a SN is

$$m_{\text{mod}} = 5 \log_{10}[H_0 D_L(z)] - \alpha(s - 1) + \beta C + \mathcal{M}, \quad (18)$$

where $D_L(z)$ can be calculated by Eq. (4), s is the stretch measure of the SN light curve shape, C is the color measure for the SN, α and β are nuisance parameters characterizing the stretch-luminosity and color-luminosity relationships, \mathcal{M} is another nuisance parameter representing some combination of the absolute magnitude of a fiducial SN and the Hubble constant. α and β are free parameters during the cosmology-fitting process. Although some works [93–96] considered β changing over time, we treat α and β as constants in this work. Introducing a vector with N components $\Delta \mathbf{m} = \Delta \mathbf{m}_B - \Delta \mathbf{m}_{\text{mod}}$ (m_B is the rest-frame peak B band magnitude of a SN), we have

$$\chi^2_{\text{SN}} = \Delta \mathbf{m}^T \cdot \mathbf{C}^{-1} \cdot \Delta \mathbf{m}, \quad (19)$$

where \mathbf{C} is the $N \times N$ covariance matrix of the SN given by [92].

3. Constraints on holographic dark energy

In a spatially flat FRW universe consisting of DE (de), matter (m) and radiation (r) (throughout this paper), for HDE with Eqs. (1) and (2), the Friedmann equation and the energy conservation equation lead to the following differential equations

$$\frac{1}{E(z)} \frac{dE(z)}{dz} = -\frac{\Omega_{\text{de}}}{1+z} \left(\frac{1}{2} + \frac{\sqrt{\Omega_{\text{de}}}}{c} - \frac{\Omega_r + 3}{2\Omega_{\text{de}}} \right), \quad (20)$$

$$\frac{d\Omega_{\text{de}}}{dz} = -\frac{2\Omega_{\text{de}}(1 - \Omega_{\text{de}})}{1+z} \left(\frac{1}{2} + \frac{\sqrt{\Omega_{\text{de}}}}{c} + \frac{\Omega_r}{2(1 - \Omega_{\text{de}})} \right), \quad (21)$$

where Ω_{de} is the fractional density of DE, and the fractional density of radiation $\Omega_r = \Omega_{r0}(1+z)^4/E(z)^2$ with $\Omega_{r0} = 2.469 \times 10^{-5} h^{-2} (1 + 0.2271 N_{\text{eff}})$ (the effective number of neutrino species $N_{\text{eff}} = 3.046$). We can obtain $E(z)$ of HDE from numerical solution of differential equations (20) and (21) with initial conditions $E_0 = 1$ and $\Omega_{\text{de}0} = 1 - \Omega_{m0} - \Omega_{r0}$ at $z = 0$. When we solve the equations, Ω_{m0} and c are free model parameters.

Firstly, we use 73 SGL data points to estimate free parameters (Ω_{m0} and c) of the HDE model in the light of the public Markov-Chain Monte Carlo package CosmoMC [97], and get the fit values $\Omega_{m0} = 0.0244^{+0.1123}_{-0.0136}$ and $c = 1.9730^{+0.0270}_{-0.8993}$ (see Table I). We can see that the best-fit of Ω_{m0} is one order smaller than current observational results. In addition, if $c > 1$, the equation of state (EoS) of HDE, $w = -\frac{1}{3}(1 + \frac{2}{c}\sqrt{\Omega_{\text{de}}})$, will be always larger than -1 due to $0 \leq \Omega_{\text{de}} \leq 1$, such that the universe avoids entering the de Sitter space-time [40]. However, a great number of previous constraints favored that c is smaller than 1, which leads to dark energy behaving as phantom whose EoS w crosses the cosmological constant boundary -1 during the evolution. The parameter c is very important to the HDE model. Furthermore, we plot the $1-2\sigma$ confidence level contours in the $\Omega_{m0}-c$ plane and one-dimensional marginalized probability distributions of Ω_{m0} and c in Fig. 1, from the SGL data. From Fig. 1, we can see that it is difficult to effectively constrain parameters Ω_{m0} and c , due to the big errors, by using SGL alone. Thus, we consider to calculate the fit value of c in the case of keeping Ω_{m0} at 0.27, and we get $c = 0.8335^{+0.8031}_{-0.3495}$. For direct comparison, we also list the fit results of c in Table I, and plot 1D marginalized probability distributions of c with free and fixed Ω_{m0} in one plane (the bottom right panel of Fig. 1). It is found that in the case with fixed Ω_{m0} , the value of c is smaller than 1, and yet its error is still quite large, which is not a satisfactory result.

Since SGL cannot constrain the parameters of HDE well, we consider to combine it with CBS (CMB+BAO+SN). For comparison, we also estimate the parameters by the CBS only data. With the CBS data, we get $\Omega_{m0} = 0.2798^{+0.0083}_{-0.0114}$ and $c = 0.6458^{+0.0472}_{-0.0483}$, and with the SGL + CBS data, we get $\Omega_{m0} = 0.2783^{+0.0092}_{-0.0100}$ and $c = 0.6429^{+0.0515}_{-0.0436}$. These results are listed in Table I. We find that, in the case with SGL + CBS, $c < 1$ is at the 6.9σ level. Moreover, the $1-2\sigma$ CL contours in the $\Omega_{m0}-c$ plane from the CBS and the combination of SGL with CBS data are shown in Fig. 2. Compared to the CBS data,

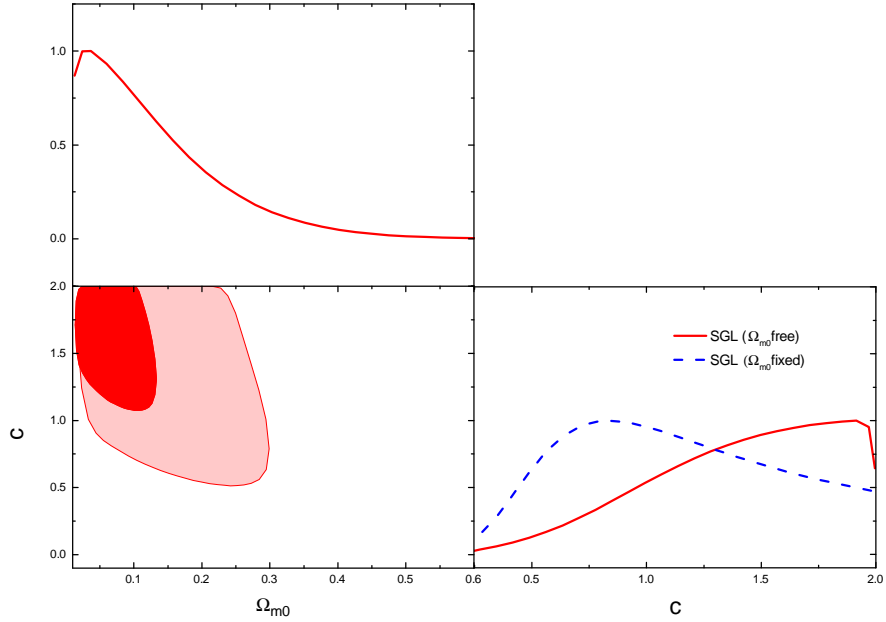


FIG. 1: Constraints on the HDE model from the SGL data. In the bottom right panel, 1D marginalized distributions of parameter c with free and fixed Ω_{m0} are presented for comparison.

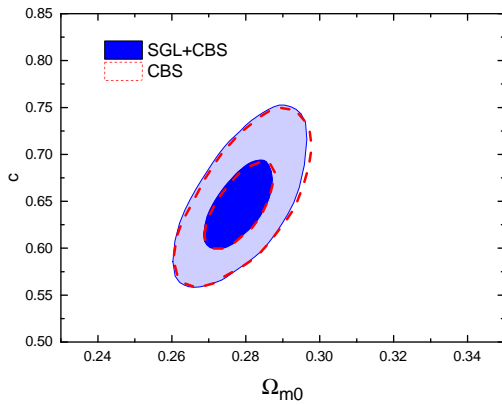


FIG. 2: The HDE model: the $1-2\sigma$ CL contours in the Ω_{m0} - c plane from CBS and the combination of SGL with CBS (CMB+BAO+SN).

the SGL+CBS data improve the constraints on Ω_{m0} and c by 3.55% and 0.15%, respectively. For the HDE model, the SGL data is helpful to tighten constraints on the parameters.

One possible cause that SGL can improve constraint precision, especially for Ω_{m0} , is that it provides some data of high-redshift source. In CBS data, there are 15 high-redshift data composed of z_* ($z > 1000$) from CMB and 14 SN ($1 \leq z \leq 1.4$) from SNLS3. Whereas, the SGL data contains 20 high-redshift sources, in which 5 sources are in the range of $1 \leq z \leq 1.4$ and 15 sources are in the range of $z > 1.4$. Owing to supplement high-redshift data, the constraints on model

parameters can improve the accuracy.

4. Comparison with the w CDM and RDE models

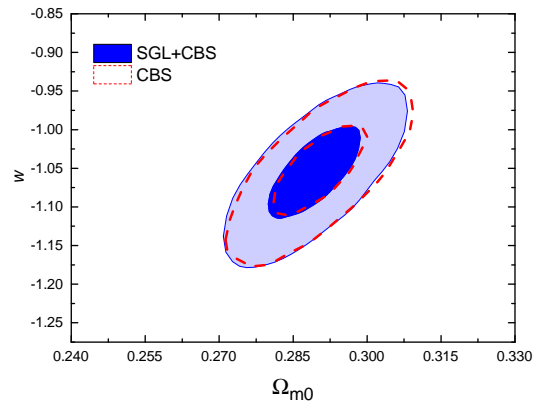


FIG. 3: The w CDM model: the $1-2\sigma$ CL contours in the Ω_{m0} - w plane from CBS and the combination of SGL with CBS (CMB+BAO+SN).

In this section, we consider the w CDM and RDE models, which have the same parameter number with the HDE model.

TABLE II: Constraint results and corresponding χ^2_{\min} for the w CDM and RDE models by using the SGL and CBS (CMB+BAO+SN) data, as well as the combination of them. In the case of fixed Ω_{m0} , we choose $\Omega_{m0} = 0.27$.

Model	w CDM			RDE		
	Ω_{m0}	w	χ^2_{\min}	Ω_{m0}	α	χ^2_{\min}
SGL(Ω_{m0} free)	$0.0259^{+0.1331}_{-0.0254}$	$-0.6537^{+0.1663}_{-0.2821}$	84.1101	$0.0159^{+0.0980}_{-0.0058}$	$0.6755^{+0.1221}_{-0.1500}$	84.1079
SGL(Ω_{m0} fixed)	0.27	$-0.9772^{+0.2920}_{-0.3812}$	86.8351	0.27	$0.4355^{+0.1240}_{-0.1018}$	88.3526
CBS	$0.2898^{+0.0106}_{-0.0093}$	$-1.0458^{+0.0535}_{-0.0660}$	425.8848	$0.2150^{+0.0071}_{-0.0070}$	$0.3108^{+0.0080}_{-0.0080}$	599.1870
SGL+CBS	$0.2891^{+0.0100}_{-0.0092}$	$-1.0546^{+0.0606}_{-0.0610}$	513.0776	$0.2153^{+0.0078}_{-0.0058}$	$0.3119^{+0.0082}_{-0.0074}$	689.5463

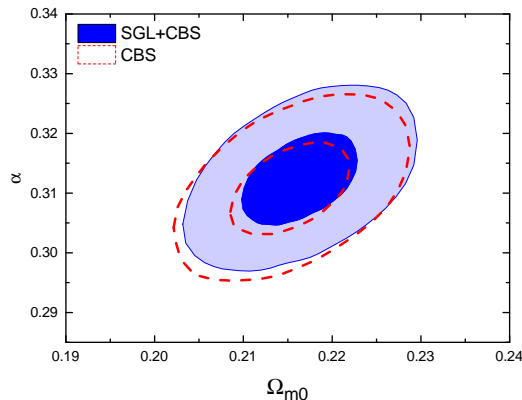


FIG. 4: The RDE model: the 1-2 σ CL contours in the Ω_{m0} - α plane from CBS and the combination of SGL with CBS (CMB+BAO+SN).

For the w CDM model, $E(z)$ is given by

$$E(z) = \sqrt{\Omega_{m0}(1+z)^3 + \Omega_{r0}(1+z)^4 + (1 - \Omega_{m0} - \Omega_{r0})(1+z)^{3(1+w)}}. \quad (22)$$

For the RDE model [85], the density of dark energy is also derived from Eq.(1). But in this case, the IR cutoff L is connected to Ricci scalar curvature, $\mathcal{R} = -6(\dot{H} + 2H^2)$. So Ricci dark energy density is

$$\rho_{de} = 3\alpha M_p^2 (\dot{H} + 2H^2), \quad (23)$$

where α is a positive constant. Accordingly, we can get

$$E(z) = \sqrt{\frac{2\Omega_{m0}}{2-\alpha}(1+z)^3 + \Omega_{r0}(1+z)^4 + (1 - \frac{2\Omega_{m0}}{2-\alpha} - \Omega_{r0})(1+z)^{4-\frac{2}{\alpha}}}. \quad (24)$$

Firstly, we use the SGL data to constrain the w CDM and RDE models with free and fixed Ω_{m0} , and obtain the fit results (see Table II). From Table II, we find that SGL only data cannot estimate parameters of the w CDM and RDE models well.

Next, we consider to use the CBS data and the combination of SGL with CBS, respectively, to constrain the model parameters and we summarize the corresponding results in Table II. For the w CDM model, the results of the joint constraints are $\Omega_{m0} = 0.2891^{+0.0100}_{-0.0092}$ and $w = -1.0546^{+0.0606}_{-0.0610}$. Further, the 1-2 σ CL contours in the Ω_{m0} - w plane for w CDM

from CBS and the combination of SGL with CBS data are shown in Fig. 3. For the RDE model, we get the constraints on Ω_{m0} and α with the SGL + CBS data, $\Omega_{m0} = 0.2153^{+0.0078}_{-0.0058}$ and $\alpha = 0.3119^{+0.0082}_{-0.0074}$, which are improved by 3% and 2.65%, respectively, relative to those with CBS only data. In Fig. 4, we plot the 1-2 σ CL contours in the Ω_{m0} - α plane for RDE from CBS and the combination of SGL with CBS data.

For the HDE, w CDM and RDE models, the values of the total χ^2_{\min} are 517.6995, 513.0776 and 689.5463, respectively, with joint SGL + CBS constraints. The HDE model fits these data slightly worse than the w CDM model, but much better than the RDE model. Hence, the HDE and w CDM models are still competitive models besides the Λ CDM model.

5. Conclusion

The strong lensing is an important tool for probing galaxies and cosmology. In this paper, we use 73 SGL data from SLACS and LSD to constrain the HDE model, as well as the w CDM and RDE models. When only the SGL data are used, for every model, the errors in constraint results are big, and the best-fit of Ω_{m0} is one order smaller than current observations. Even if we fix the value of Ω_{m0} at 0.27, the errors of another parameter is still big. That is to say, using the SGL data alone cannot constrain the parameters of model well. However, when the SGL data are combined with CBS (CMB+BAO+SN) data, we get some reasonable results. In the HDE model, we obtain $\Omega_{m0} = 0.2783^{+0.0092}_{-0.0100}$ and $c = 0.6429^{+0.0515}_{-0.0436}$. Particularly, the constraints on Ω_{m0} and c with the SGL + CBS data are improved by 3.55% and 0.15% respectively, compared with those with the CBS data. The same situations also occur in the w CDM and RDE models. In the w CDM model, with the SGL + CBS constraints, we have $\Omega_{m0} = 0.2891^{+0.0100}_{-0.0092}$ and $w = -1.0546^{+0.0606}_{-0.0610}$. And, in the RDE model, with the SGL + CBS constraints, $\Omega_{m0} = 0.2153^{+0.0078}_{-0.0058}$ and $\alpha = 0.3119^{+0.0082}_{-0.0074}$ are improved by 3% and 2.65%, respectively, relative to the CBS constraints. The reason why SGL can tighten constraints in some sense is that it provides some high-redshift data that are important supplementary for the CBS data. Therefore, we conclude that SGL can be helpful to obtain tighter constraints on model parameters. Moreover, in terms of the constraints on the HDE

model, $c < 1$ is at the 6.9σ level with the SGL + CBS data. According to this result, HDE is likely to become a phantom energy in the future evolution. Through a χ^2_{\min} comparison, we conclude that the HDE model is still one of competitive DE models.

Acknowledgements

This work was supported by the National Natural Science Foundation of China under Grants No. 11175042 and No.

11522540, the Provincial Department of Education of Liaoning under Grant No. L2012087, and the Fundamental Research Funds for the Central Universities under Grants No. N140505002, No. N140506002, and No. N140504007.

-
- [1] Riess A G, *et al.*, [Supernova Search Team Collaboration]. Observational evidence from supernovae for an accelerating universe and a cosmological constant. *Astron J*, 1998, 116: 1009-1038
- [2] Perlmutter S, *et al.*, [Supernova Cosmology Project Collaboration]. Measurements of Omega and Lambda from 42 high redshift supernovae. *Astrophys J*, 1999, 517: 565-586
- [3] Tegmark M, *et al.*, [SDSS Collaboration]. Cosmological parameters from SDSS and WMAP. *Phys Rev D*, 2004, 69: 103501
- [4] Eisenstein D J, *et al.*, [SDSS Collaboration]. Detection of the baryon acoustic peak in the large-scale correlation function of SDSS luminous red galaxies. *Astrophys J*, 2005, 633: 560-574
- [5] Spergel D N, *et al.*, [WMAP Collaboration]. First year Wilkinson Microwave Anisotropy Probe (WMAP) observations: determination of cosmological parameters. *Astrophys J Suppl*, 2003, 148: 175-194
- [6] Sahni V, Starobinsky A A. The case for a positive cosmological Lambda term. *Int J Mod Phys D*, 2000, 9: 373-444
- [7] Padmanabhan T. Cosmological constant: the weight of the vacuum. *Phys Rept*, 2003, 380: 235-320
- [8] Bean R, Carroll S M, Trodden M. Insights into dark energy: interplay between theory and observation. *astro-ph/0510059*.
- [9] Copeland E J, Sami M, Tsujikawa S. Dynamics of dark energy. *Int J Mod Phys D*, 2006, 15: 1753-1936
- [10] Sahni V, Starobinsky A. Reconstructing dark energy. *Int J Mod Phys D*, 2006, 15: 2105-2132
- [11] Li M, Li X D, Wang S, Wang Y. Dark energy. *Commun Theor Phys*, 2011, 56: 525-604
- [12] Peebles P J E, Ratra B. Cosmology with a time variable cosmological 'constant'. *Astrophys J*, 1988, 325: L17-L20
- [13] Ratra B, Peebles P J E. Cosmological consequences of a rolling homogeneous scalar field. *Phys Rev D*, 1988, 37: 3406
- [14] Caldwell R R. A Phantom menace? *Phys Lett B*, 2002, 545: 23-29
- [15] Zhang X. An interacting two-fluid scenario for quintom dark energy. *Commun Theor Phys*, 2005, 44: 762-768
- [16] Zhang X. Coupled quintessence in a power-law case and the cosmic coincidence problem. *Mod Phys Lett A*, 2005, 20: 2575-2582
- [17] Sen A. Tachyon matter. *JHEP*, 2002, 07: 065
- [18] Arkani-Hamed N, Cheng H C, Luty M A, Mukohyama S. Ghost condensation and a consistent infrared modification of gravity. *JHEP*, 2004, 05: 074
- [19] Zhang J F, Zhang X, Liu H Y. Reconstructing generalized ghost condensate model with dynamical dark energy parametrizations and observational datasets. *Mod Phys Lett A*, 2008, 23: 139-152
- [20] Wei H, Cai R G. A new model of agegraphic dark energy. *Phys Lett B*, 2008, 660: 113-117
- [21] Kamenshchik A Y, Moschella U, Pasquier V. An alternative to quintessence. *Phys Lett B*, 2001, 511: 265-268
- [22] Bento M C, Bertolami O, Sen A A. Generalized Chaplygin gas, accelerated expansion and dark energy matter unification. *Phys Rev D*, 2002, 66: 043507
- [23] Zhang X, Wu F Q, Zhang J. New generalized Chaplygin gas as a scheme for unification of dark energy and dark matter. *J Cosmo Astropart Phys*, 2006, 0601: 003
- [24] Chevallier M, Polarski D. Accelerating universes with scaling dark matter. *Int J Mod Phys D*, 2001, 10: 213-224
- [25] Linder E V. Exploring the expansion history of the universe. *Phys Rev Lett*, 2003, 90: 091301
- [26] Ma J Z, Zhang X. Probing the dynamics of dark energy with novel parametrizations. *Phys Lett B*, 2011, 699: 233-238
- [27] Li X D, Wang S, Huang Q G, Zhang X, Li M. Dark energy and fate of the universe. *Sci China-Phys Mech Astron*, 2012, 55: 1330-1334
- [28] Li M, Li X D, Wang S, Wang Y. Dark energy: a brief review. *Front Phys China*, 2013, 8: 828-846
- [29] Li Y H, Zhang J F, Zhang X. Parametrized post-Friedmann framework for interacting dark energy. *Phys Rev D*, 2014, 90: 063005
- [30] Li Y H, Zhang J F, Zhang X. Exploring the full parameter space for an interacting dark energy model with recent observations including redshift-space distortions: application of the parametrized post-Friedmann approach. *Phys Rev D*, 2014, 90: 123007
- [31] Zhang M, Sun C Y, Yang Z Y, et al. Cosmological evolution of quintessence with a sign-changing interaction in dark sector. *Sci China-Phys Mech Astron*, 2014, 57: 1805C1808
- [32] Zhang J F, Zhao M M, Cui J L, Zhang X. Revisiting the holographic dark energy in a non-flat universe: alternative model and cosmological parameter constraints. *Eur Phys J C*, 2014, 74: 3178
- [33] Hu Y Z, Li M, Li X D, et al. Investigating the possibility of a turning point in the dark energy equation of state. *Sci China-Phys Mech Astron*, 2014, 57: 1607C1612
- [34] Zhang J F, Zhao M M, Li Y H, Zhang X. Neutrinos in the holographic dark energy model: constraints from latest measurements of expansion history and growth of structure. *J Cosmo Astropart Phys*, 2015, 1504: 038
- [35] Lu J B, Chen L D, Xu L X, et al. Comparing the VGCG model as the unification of dark sectors with observations. *Sci China-Phys Mech Astron*, 2014, 57: 796C800
- [36] Geng J J, Zhang J F, Zhang X. Quantifying the impact of future

- Sandage-Loeb test data on dark energy constraints. *J Cosmo Astropart Phys*, 2014, 1407: 006
- [37] Zhang J F, Zhao L A, Zhang X. Revisiting the interacting model of new agegraphic dark energy. *Sci China-Phys Mech Astron*, 2014, 57: 387-392
- [38] Zhang J F, Geng J J, Zhang X. Neutrinos and dark energy after Planck and BICEP2: data consistency tests and cosmological parameter constraints. *J Cosmo Astropart Phys*, 2014, 1410: 044
- [39] Levrino L, Tartaglia A. From the elasticity theory to cosmology and vice versa. *Sci China-Phys Mech Astron*, 2014, 57: 597-603
- [40] Li M. A model of holographic dark energy. *Phys Lett B*, 2004, 603: 1-5
- [41] Cohen A G, Kaplan D B, Nelson A E. Effective field theory, black holes, and the cosmological constant. *Phys Rev Lett*, 1999, 82: 4971-4974
- [42] Huang Q G, Li M. Anthropic principle favors the holographic dark energy. *J Cosmo Astropart Phys*, 2005, 0503: 001
- [43] Zhang X. Statefinder diagnostic for holographic dark energy model. *Int J Mod Phys D*, 2005, 14: 1597-1606
- [44] Zhang X. Dynamical vacuum energy, holographic quintom, and the reconstruction of scalar-field dark energy. *Phys Rev D*, 2006, 74: 103505
- [45] Zhang X. Reconstructing holographic quintessence. *Phys Lett B*, 2007, 648: 1-7
- [46] Zhang J F, Zhang X, Liu H Y. Holographic tachyon model. *Phys Lett B*, 2007, 651: 84-88
- [47] Zhang J F, Zhang X, Liu H Y. Holographic dark energy in a cyclic universe. *Eur Phys J C*, 2007, 52: 693-699
- [48] Ma Y Z, Zhang X. Possible theoretical limits on holographic quintessence from weak gravity conjecture. *Phys Lett B*, 2008, 661: 239-245
- [49] Li M, Lin C, Wang Y. Some issues concerning holographic dark energy. *J Cosmo Astropart Phys*, 2008, 0805: 023
- [50] Cui J, Zhang X. Cosmic age problem revisited in the holographic dark energy model. *Phys Lett B*, 2010, 690: 233-238
- [51] Zhang X. Heal the world: Avoiding the cosmic doomsday in the holographic dark energy model. *Phys Lett B*, 2010, 683: 81-87
- [52] Li M, Wang Y. Quantum UV/IR relations and holographic dark energy from entropic force. *Phys Lett B*, 2010, 687: 243-247
- [53] Zhang X, Wu F Q. Constraints on holographic dark energy from Type Ia supernova observations. *Phys Rev D*, 2005, 72: 043524
- [54] Zhang X, Wu F Q. Constraints on holographic dark energy from latest supernovae, galaxy clustering, and cosmic microwave background anisotropy observations. *Phys Rev D*, 2007, 76: 023502
- [55] Chang Z, Wu F Q, Zhang X. Constraints on holographic dark energy from x-ray gas mass fraction of galaxy clusters. *Phys Lett B*, 2006, 633: 14-18
- [56] Huang Q G, Gong Y G. Supernova constraints on a holographic dark energy model. *J Cosmo Astropart Phys*, 2004, 0408: 006
- [57] Wang B, Abdalla E, Su R K. Constraints on the dark energy from holography. *Phys Lett B*, 2005, 611: 21-26
- [58] Ma Y Z, Gong Y, Chen X. Features of holographic dark energy under the combined cosmological constraints. *Eur Phys J C*, 2009, 60: 303-315
- [59] Li M, Li X D, Wang S, Zhang X. Holographic dark energy models: a comparison from the latest observational data. *J Cosmo Astropart Phys*, 2009, 0906: 036
- [60] Li M, Li X D, Wang S, Wang Y, Zhang X. Probing interaction and spatial curvature in the holographic dark energy model. *J Cosmo Astropart Phys*, 2009, 0912: 014
- [61] Li M, Li X, Zhang X. Comparison of dark energy models: a perspective from the latest observational data. *Sci China-Phys Mech Astron*, 2010, 53: 1631-1645
- [62] Li M, Li X D, Ma Y Z, Zhang X, Zhang Z. Planck constraints on holographic dark energy. *J Cosmo Astropart Phys*, 2013, 1309: 021
- [63] Li Y H, Wang S, Li X D, Zhang X. Holographic dark energy in a Universe with spatial curvature and massive neutrinos: a full Markov Chain Monte Carlo exploration. *J Cosmo Astropart Phys*, 2013, 1302: 033
- [64] Duan X X, Li Y C, Gao C J. Constraining the Lattice Fluid Dark Energy from SNe Ia, BAO and OHD. *Sci China-Phys Mech Astron*, 2013, 56: 1220-1226
- [65] Walsh D, Carswell R F, Weymann R J. 0957 + 561 A, B - Twin quasistellar objects or gravitational lens. *Nature*, 1979, 279: 381-384
- [66] Zhu Z H, Wu X P. A remark on the inversion of the magnification bias in the quasar-galaxy associations. *Astron Astrophys*, 1997, 324: 483
- [67] Mao S D, Schneider P. Evidence for substructure in lens galaxies? *Mon Not Roy Astron Soc*, 1998, 295: 587-594
- [68] Jin K J, Zhang Y Z, Zhu Z H. Gravitational lensing effects of fermion fermion stars: 1. Strong field case. *Phys Lett A*, 2000, 264: 335-340
- [69] Keeton C R. Cdm and strong lensing: concord or conflict? *Astrophys J*, 2001, 561: 46-60
- [70] Kochanek C S, White M J. Global probes of the impact of baryons on dark matter halos. *Astrophys J*, 2001, 559: 531-543
- [71] Ofek E O, Rix H W, Maoz D. The redshift distribution of gravitational lenses revisited: constraints on galaxy mass evolution. *Mon Not Roy Astron Soc*, 2003, 343: 639-652
- [72] Treu T, Koopmans L, Bolton A, Burles S, Moustakas L. The sloan-lens acs survey. 2. stellar populations and internal structure of early-type lens galaxies. *Astrophys J*, 2006, 640: 662-672
- [73] Zhu Z H. Gravitational lensing statistics as a probe of dark energy. *Mod Phys Lett A*, 2000, 15: 1023-1029
- [74] Zhu Z H. Gravitational lensing statistical properties in general FRW cosmologies with dark energy component(s): Analytic results. *Int J Mod Phys D*, 2000, 9: 591-600
- [75] Chae K H. The Cosmic Lens All Sky Survey statistical lensing, cosmologies, and global properties of galaxy populations. *Mon Not Roy Astron Soc*, 2003, 346: 746-772
- [76] Chae K H, Chen G, Ratra B, Lee D W. Constraints on scalar - field dark energy from the Cosmic Lens All - Sky Survey gravitational lens statistics. *Astrophys J*, 2004, 607: L71-L74
- [77] Mitchell J L, Keeton C R, Frieman J A, Sheth R K. Robust cosmological constraints from gravitational lens statistics. *Astrophys J*, 2005, 622: 81-98
- [78] Zhu Z H, Sereno M. Testing the DGP model with gravitational lensing statistics *Astron Astrophys*, 2008, 487: 831-835
- [79] Zhu Z H, Hu M, Alcaniz J S, Liu Y X. Testing power-law cosmology with galaxy clusters. *Astron Astrophys*, 2008, 483: 15-18
- [80] Cao S, Covone G, Zhu Z H. Testing the dark energy with gravitational lensing statistics. *Astrophys J*, 2012, 755: 31
- [81] Cao S, Zhu Z H. Constraints on cosmological models from lens redshift data. *Astron Astrophys*, 2012, 538: A43
- [82] Liao K, Zhu Z H. Constraints on $f(R)$ cosmologies from strong gravitational lensing systems. *Phys Lett B*, 2012, 714: 1-5
- [83] Wu J, Li Z, Wu P, Yu H. Constrains on $f(T)$ gravity with the strong gravitational lensing data. *Sci China-Phys Mech Astron*, 2014, 57: 988-993.
- [84] Chen Y, Geng C Q, Cao S, Huang Y M, Zhu Z H. Constraints on a ϕ CDM model from strong gravitational lensing and

- updated Hubble parameter measurements. *J Cosmo Astropart Phys*, 2015, 1502: 010
- [85] Gao C, Wu F Q, Chen X, Shen Y G. A holographic dark energy model from Ricci scalar curvature. *Phys Rev D*, 2009, 79: 043511
- [86] Wang Y, Wang S. Distance Priors from Planck and Dark Energy Constraints from Current Data. *Phys Rev D*, 2013, 88: 043522
- [87] Hu W, Sugiyama N. Small scale cosmological perturbations: An Analytic approach. *Astrophys J*, 1996, 471: 542-570
- [88] Eisenstein D J, Hu W. Baryonic features in the matter transfer function. *Astrophys J*, 1998, 496: 605-614
- [89] Beutler F, Blake C, Colless M, Jones D H, Staveley-Smith L, Campbell L, Parker Q, Saunders W, Watson F. The 6dF Galaxy Survey: Baryon Acoustic Oscillations and the local Hubble constant. *Mon Not Roy Astron Soc*, 2011, 416: 3017-3032
- [90] Padmanabhan N, Xu X, Eisenstein D J, Scalzo R, Cuesta A J, Mehta K T, Kazin E. A 2 per cent distance to $z=0.35$ by reconstructing baryon acoustic oscillations - I. Methods and application to the Sloan Digital Sky Survey. *Mon Not Roy Astron Soc*, 2012, 427: 3, 2132-2145
- [91] Kazin E A, Koda J, Blake C, Padmanabhan N. The WiggleZ Dark Energy Survey: improved distance measurements to $z = 1$ with reconstruction of the baryonic acoustic feature. *Mon Not Roy Astron Soc*, 2014, 441: 4, 3524-3542
- [92] Conley A, *et al.*, [SNLS Collaboration]. Supernova constraints and systematic uncertainties from the first 3 years of the Supernova Legacy Survey. *Astrophys J Suppl*, 2011, 192: 1
- [93] Wang S, Wang Y. Exploring the systematic uncertainties of type Ia supernovae as cosmological probes. *Phys Rev D*, 2013, 88: 043511
- [94] Wang S, Li Y H, Zhang X. Exploring the evolution of color-luminosity parameter β and its effects on parameter estimation. *Phys Rev D*, 2014, 89: 063524
- [95] Wang S, Wang Y Z, Geng J J, Zhang X. Effects of time-varying β in SNLS3 on constraining interacting dark energy models. *Eur Phys J C*, 2014, 74: 11, 3148
- [96] Wang S, Geng J J, Hu Y L, Zhang X. Revisit of constraints on holographic dark energy: SNLS3 dataset with the effects of time-varying β and different light-curve fitters. *Sci China-Phys Mech Astron*, 2015, 58: 019801
- [97] Lewis A, Bridle S. Cosmological parameters from CMB and other data: a Monte Carlo approach. *Phys Rev D*, 2002, 66: 103511